Asian Journal of Environmental Research
E-ISSN: 3047-4930
DOI: https://doi.org/10.69930/ajer.v3i2.741
Research Article

ScienceTech. Group

Vol. 3 (2), 2026
Page: 130-146

Mapping Potential Fishing Zones as Indicators of Pelagic Ecosystem Service Hotspots in the Makassar Strait using Satellite-Derived SST and Chlorophyll-a Anomalies

Ummu Salma [1,*], Fadil Apresia [1,2]

[1] Department of Marine Science, Faculty of Fisheries and Marine Science, Universitas Diponegoro, Jl. Prof. Jacub Rais, Tembalang, Semarang, Central Java 50275, Indonesia
[2] Fisheries and Marine Technology and Business Study Program, Department of Fishery Product Technology, Faculty of Fisheries and Marine Science, Universitas Diponegoro, Jepara, Central Java, Indonesia
*Email (corresponding author): ummusalma@lecturer.undip.ac.id

Abstract. *This study developed an anomaly-based framework to map potential fishing zones (PFZs) in the Makassar Strait from satellite-derived sea surface temperature (SST) and chlorophyll-a (Chl-a) during 2022–2024. Daily GCOM-C/SGLI Level-3 Version 3 products were quality-masked, converted to physical units, aggregated to a 0.1° × 0.1° grid, and summarized as monthly composites. Monthly anomalies were then calculated relative to a month-specific three-year climatology. PFZs were defined as pixels simultaneously showing high Chl-a anomalies, represented by the 80th percentile of the spatial distribution of the temporal mean anomaly field, and relative cooling (SST anomaly ≤ 0). Monthly PFZ area ranged from 4,658 to 144,923 km², with a mean of 52,606 ± 33,834 km², whereas PFZ area fraction ranged from 0.012 to 0.352, with a mean of 0.130 ± 0.084. Seasonally, PFZs were most extensive during JJA (mean 66,973 km²; fraction 0.161) and least extensive during DJF (43,046 km²; fraction 0.112). Recurrent PFZ hotspots were concentrated in the central-southern Makassar Strait and along the eastern sector near the Sulawesi coast, where occurrence frequency reached about 58%. Valid-pixel diagnostics showed relatively stable AOI-level coverage (SST mean 0.534; Chl-a mean 0.548), indicating that the observed PFZ variability could not be explained by data gaps alone. These findings indicate that recurrent PFZs can be interpreted as pelagic ecosystem service hotspots that support ecosystem-based fisheries management, biodiversity conservation, and the sustainable use of marine resources, while aligning with SDG 14 (Life Below Water) and the post-2020 global biodiversity framework of the Convention on Biological Diversity.*

Keywords: *Potential Fishing Zone; Ecosystem Services; Pelagic Habitat; Chlorophyll-A Anomaly; Makassar Strait*

1. Introduction

Ecosystem-based fisheries management requires spatially explicit knowledge of the environmental processes that structure fish habitat. In dynamic tropical seas, pelagic fish do not occupy the same locations continuously, but track temporally varying thermal fronts, productivity gradients, and water-mass boundaries. Potential fishing zone (PFZ) mapping therefore provides an operational way to translate satellite observations into synoptic habitat indicators that can support fisheries assessment, exploratory fishing, and dynamic management.

Among satellite-derived variables, SST and chlorophyll-a are two of the most informative habitat proxies for pelagic fishes. SST reflects the thermal structure of the surface

Received: 30 April 2026 / Accepted: 6 June 2026 / Available online: 8 June 2026

ocean, frontal activity, and the interaction among water masses, whereas chlorophyll-a represents phytoplankton biomass and, by extension, the lower-trophic-level productivity that may propagate upward through zooplankton and forage organisms to support pelagic predators. Previous fisheries-oceanography studies have repeatedly shown that pelagic fish aggregations tend to occur near the joint expression of suitable thermal conditions and productive waters (1-4).

Remote-sensing applications in Indonesian waters also show that tuna and other pelagic resources respond to combinations of SST, chlorophyll-a, and dynamically evolving habitat structures. In the Makassar Strait, recent fisheries modelling has further confirmed that oceanographic variability plays an important role in shaping the distribution of exploited pelagic resources (5). These findings support the use of SST and chlorophyll-a as first-order indicators for identifying areas with recurrent pelagic habitat potential.

However, PFZ studies based only on absolute SST or chlorophyll-a values can overlook whether observed conditions are genuinely unusual for a given season. In monsoon-regulated tropical seas, the environmental background shifts strongly throughout the year. A value that appears high in one season may be normal in another. An anomaly-based framework relative to month-specific climatology is therefore more informative because it highlights departures from the expected seasonal state rather than raw magnitude alone (6,7).

Percentile thresholds provide an additional advantage when the environmental distribution is skewed or non-normal. Rather than imposing a fixed chlorophyll-a cutoff with the same ecological meaning everywhere and at all times, percentile-based thresholds adapt to the local anomaly distribution and emphasize relatively persistent high-productivity conditions. This logic is consistent with broader oceanographic practice, where anomaly and percentile approaches are widely used to detect marine extremes and spatially coherent habitat features (8,9).

The Makassar Strait is an especially relevant setting for this approach. It is the primary inflow pathway of the Indonesian Throughflow (ITF), linking the tropical Pacific and Indian Oceans and shaping regional heat, mass, and nutrient transport (10,11). Recent analyses continue to identify the Makassar Strait as the dominant ITF passage and emphasize its strong seasonal and interannual variability (12). This circulation interacts with monsoonal forcing to generate spatially heterogeneous cooling, mixing, and productivity responses that are directly relevant to pelagic fisheries in the region.

Despite this oceanographic importance, studies that systematically map PFZs in the Makassar Strait using monthly environmental anomalies and spatial percentile thresholds remain limited. In addition, PFZ studies in tropical waters often under-report the influence of cloud-driven data loss, even though incomplete observation coverage can bias the interpretation of ocean-color products (13). As a result, there remains a need for a PFZ framework that is both ecologically interpretable and explicit about data coverage.

This study addresses that need by developing a reproducible PFZ-mapping workflow based on monthly SST and chlorophyll-a anomalies derived from GCOM-C/SGLI Level-3 data for 2022–2024. Specifically, the study aims to (1) quantify the seasonal and interannual variability of anomaly-based PFZ area and fraction, (2) identify recurrent PFZ hotspots in the Makassar Strait, and (3) evaluate whether the inferred PFZ dynamics are robust to data-coverage variability and reasonable changes in threshold choice. By doing so, the study contributes a transparent anomaly-based framework for identifying recurrent pelagic

habitat and fishery provisioning ecosystem-service hotspots in a dynamically forced Indonesian strait, thereby strengthening its relevance to ecosystem services and biodiversity-oriented marine management.

In the context of environmental sciences, PFZ mapping can also be viewed as a tool for assessing the spatial and temporal variability of marine ecosystem services. Areas where enhanced productivity and suitable thermal conditions repeatedly co-occur may represent zones of elevated fishery provisioning service, while also functioning as dynamic pelagic habitats that support trophic transfer and mobile marine consumers. Therefore, identifying recurrent PFZs is relevant not only for fisheries operations, but also for ecosystem-based management, biodiversity-conscious spatial planning, and the sustainable use of marine resources. In addition, anomaly-based habitat indicators can support climate-adaptive fisheries management by helping identify dynamic and potentially climate-resilient fishing grounds under seasonal variability and long-term ocean change, thereby strengthening sustainable fisheries responses to climate variability.

2. Methods

2.1. **Study Area and Analysis Parameters**

The study area covered the Makassar Strait between 115°E–121°E and 5°S–1°N. This domain spans the principal ITF pathway and includes the central-to-southern sector where seasonal cooling and productivity enhancement are most pronounced. The analysis period extended from 1 January 2022 to 31 December 2024 and yielded 36 monthly composites. This window was selected to provide a recent and internally consistent three-year record from the same product generation while remaining long enough to construct a month-specific baseline for anomaly analysis. All SST and chlorophyll-a data were aligned to a regular 0.1° × 0.1° geographic grid in WGS 84 (EPSG:4326). PFZ area was calculated using geodesic area rather than a constant pixel-area approximation so that latitudinal changes in cell area were explicitly accommodated.

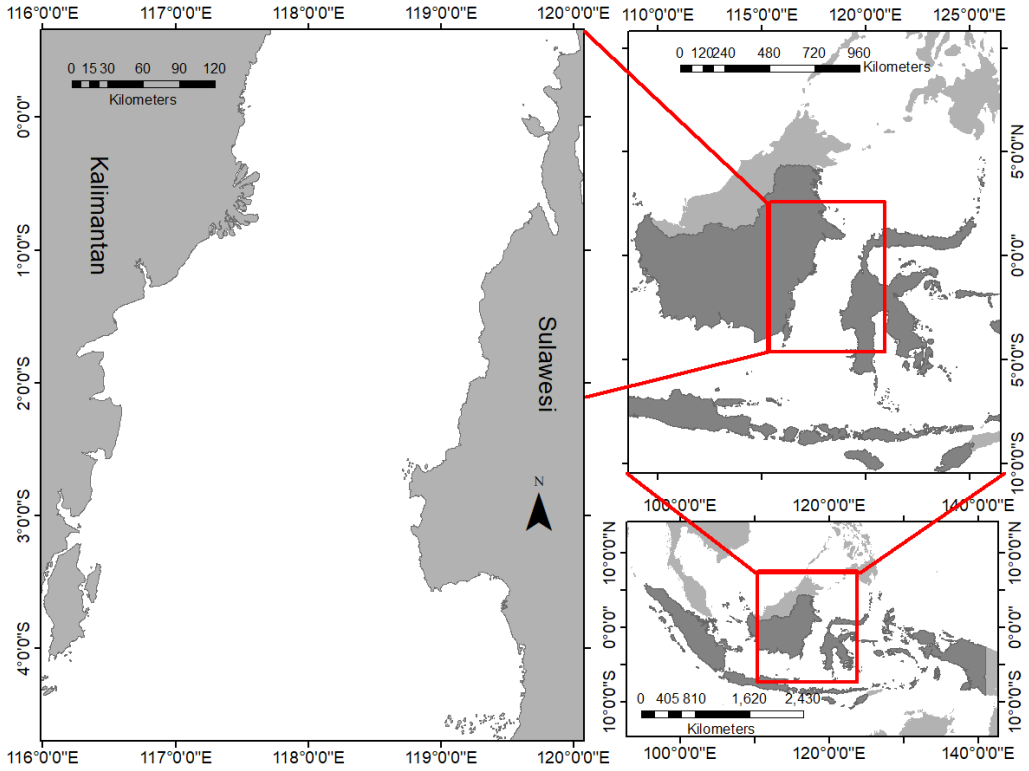

Figure 1. Map of the study area in the Makassar Strait

2.2 Satellite Data and Pre-processing

Daily GCOM-C/SGLI Level-3 Version 3 products for chlorophyll-a and SST were used in this study. The Version 3 product series has been distributed through the JAXA G-Portal since late 2021, and product documentation is provided through the official SHIKISAI/GCOM-C information pages (14,15). The SGLI sensor was designed for long-term monitoring of oceanic and terrestrial environmental variables, and its SST and ocean-color products have been evaluated in several methodological studies (16-18). In this study, technical specifications, quality flags, and scale coefficients followed the official JAXA documentation for the distributed products (19).

2.3 Water-Pixel Masking

Marine pixels were separated from land and mixed land-water pixels using the terrain-type information embedded in the GCOM-C/SGLI quality-assurance (QA) layer. Specifically, the two least significant bits were extracted through a bitwise AND operation to identify terrain categories. Pixels flagged as water or mostly water were retained, whereas non-marine pixels were removed from further analysis. This QA-based masking step is standard practice in ocean-color processing because it reduces contamination from land adjacency and invalid retrievals and provides a transparent basis for subsequent valid-pixel diagnostics (13,20).

$$T(x, y, t) = \mathrm{QA}(x, y, t)\ \&\ 3 \qquad (1)$$

In Equation (1), denotes the quality-assurance value at the pixel with coordinates at time . The symbol is the bitwise AND operator used to extract the two least significant bits representing the terrain-type category. Values of range from 0 to 3, where 0 and 1 represent water and mostly water pixels. The sea mask is defined as a binary function:

$$M_{\text{water}}(x, y, t) = \begin{cases} 1, & T(x, y, t) \in \{0,1\} \\ 0, & \text{other} \end{cases} \qquad (2)$$

In Equation (2), equals 1 for marine pixels retained in the analysis and 0 for non-marine pixels removed from the analysis. This QA-flag-based masking procedure is standard practice in ocean-color processing to ensure observation quality (13,20).

2.4 Conversion of Digital Values to Physical Units

Digital values in the chlorophyll-a and SST bands were converted to physical units using the official product scale coefficients supplied with the Level-3 products (19). This conversion was applied before spatial aggregation so that all subsequent statistics were computed in physically meaningful units. The converted monthly mean SST values in the AOI ranged from 28.978 to 30.133 °C, whereas monthly mean chlorophyll-a ranged from 0.374 to 0.805 mg m^{-3}, confirming that the resulting values fall within a realistic range for tropical Indonesian waters.

$$\mathrm{Chl}(x,y,t) = 0.0016 \cdot \mathrm{CHLA\_AVE}(x,y,t) \qquad (3)$$

$$\mathrm{SST}(x,y,t) = 0.0012 \cdot \mathrm{SST\_AVE}(x,y,t) - 10 \qquad (4)$$

In Equation (3), denotes chlorophyll-a concentration (), whereas CHLA_AVE(x,y,t) is the digital value in the Level-3 band. In Equation (4), denotes sea surface temperature (°C) derived from the digital value SST_AVE(x,y,t). Conversion based on scale coefficients is a standard procedure in Level-3 product analysis (13).

2.5 Spatial Resolution Aggregation

To reduce high-frequency noise and improve the stability of monthly environmental fields, daily data were aggregated to the 0.1° × 0.1° analysis grid using an area-weighted mean. This approach preserves the contribution of partially overlapping source pixels and is preferable to simple nearest-neighbour assignment when integrating gridded satellite products with different support areas. Area-weighted aggregation is also consistent with standard geospatial reprojection and resampling practice in remote-sensing analysis (21,22).

$$V^c(p,t) = \frac{\sum_{i\in\Omega(p)} w_i \; V(i,t)}{\sum_{i\in\Omega(p)} w_i} \qquad (5)$$

In Equation (5), is the value of or at the ith native-resolution pixel, whereas is the variable value at output pixel on the aggregation grid. The set includes all input pixels that spatially intersect output pixel , and the weight represents the fractional area of overlap between the input and output pixels. This area-weighted aggregation principle is consistent with reprojection and resampling methods commonly used in satellite-image analysis (21,22).

2.6 Monthly Composites

Monthly composites were calculated as the mean of all valid daily observations within each month of each year. No temporal interpolation was applied to replace missing daily observations caused by cloud cover or QA masking. Consequently, each monthly composite represents the best available monthly mean from the retained observations, while the associated valid-pixel fraction was reported separately to evaluate the influence of data coverage on interpretation.

$$V_{y,m}(x,y) = \frac{1}{|\mathcal{D}_{y,m}|} \sum_{t\in\mathcal{D}_{y,m}} V^c(x,y,t) \qquad (6)$$

This monthly compositing strategy suppresses short-term weather noise while preserving the seasonal signal that is most relevant for the PFZ analysis. Because daily data availability can vary among months, the number of contributing observations was allowed to change through

time, and uncertainty linked to observation density was examined indirectly through the monthly valid-pixel diagnostics presented in the Results section.

2.7 Monthly Climatology and Anomalies

The climatology for each calendar month was calculated as the interannual mean of the corresponding monthly composites from 2022–2024. In this study, the term climatology therefore refers to a recent month-of-year baseline within the analysis window rather than a multi-decadal normal. Because the analysis covered only 2022–2024, the term "climatology" in this study refers to a short-term month-specific baseline rather than a long-term climate normal. This definition is appropriate for highlighting seasonal departures within the available record and for constructing internally consistent anomalies across months.

$$\overline{V}_m(x,y) = \frac{1}{N_m}\sum_{y} V_{y,m}(x,y) \qquad (7)$$

In Equation (7), denotes the number of years within the analysis period contributing to that month.

Monthly anomalies were then calculated as:

$$V'_{y,m}(x,y) = V_{y,m}(x,y) - \overline{V}_m(x,y) \qquad (8)$$

Monthly anomalies were then computed by subtracting the corresponding month-specific climatological mean from each monthly composite. Positive chlorophyll-a anomalies indicate conditions that are more productive than the recent seasonal baseline, whereas negative SST anomalies indicate relative cooling compared with the expected condition of the same calendar month. This month-of-year anomaly framework is widely used in studies of ocean variability and marine extremes because it preserves seasonality while isolating departures from normal conditions (7,9).

2.8 Determination of the Spatial Percentile Threshold

The temporal mean of chlorophyll-a anomalies was calculated as:

$$\overline{\mathrm{Chl}'}(x,y) = \frac{1}{T}\sum_{y,m} \mathrm{Chl}'_{y,m}(x,y) \qquad (9)$$

where is the total number of months in the study period (36 months).

The threshold for high anomalies was determined using the 80th percentile:

$$\theta_{\mathrm{Chl}} = Q_{80}\left(\overline{\mathrm{Chl}'}(x,y)\right) \qquad (10)$$

The threshold for high chlorophyll-a anomalies was defined as the 80th percentile of the spatial distribution of the temporal mean anomaly field across all AOI pixels. This choice was intended to emphasize areas that repeatedly exhibited relatively elevated productivity compared with their seasonal baseline, while avoiding over-sensitivity to short-lived extremes. In other words, the selected threshold identifies spatially persistent productive tendencies rather than isolated monthly spikes. Because percentile thresholds are distribution-adaptive, they are also less vulnerable than fixed cutoffs when anomaly fields are skewed or heterogeneous (8).

2.9 Potential Fishing Zone (PFZ) Classification

PFZs were defined as pixels meeting two simultaneous conditions:

$$\mathrm{PFZ}_{y,m}(x,y) = \mathbf{1}\left[\mathrm{Chl}'_{y,m}(x,y) \geq \theta_{\mathrm{Chl}}\right] \cdot \mathbf{1}\left[\mathrm{SST}'_{y,m}(x,y) \leq 0\right] \qquad (11)$$

PFZs were classified as pixels satisfying two simultaneous conditions: elevated chlorophyll-a anomaly and non-positive SST anomaly. This combination was selected to represent areas where enhanced surface productivity co-occurred with relative cooling, two conditions that frequently accompany frontal activity, mixing, or upwelling-related habitat enhancement in pelagic systems. The SST anomaly threshold of ≤ 0 was intentionally conservative: it identifies cooling relative to the seasonal baseline without assuming that one fixed cooling magnitude carries the same ecological significance across all months and years. Additional cooling thresholds were evaluated through sensitivity analysis.

2.10 PFZ Frequency, Area, and Fraction

PFZ occurrence frequency was calculated as:

$$\mathrm{PFZ}_{\mathrm{freq}}(x,y) = 100 \cdot \frac{1}{T}\sum_{y,m} \mathrm{PFZ}_{y,m}(x,y) \qquad (12)$$

This value represents the percentage occurrence of PFZs over the study period and is consistent with the concept of habitat persistence in dynamic spatial management (6).

Monthly PFZ area was calculated as:

$$A_{y,m} = \frac{1}{10^{6}} \sum_{(x,y)\in \mathrm{AOI}} \mathrm{PFZ}_{y,m}(x,y) \cdot \mathrm{Area}(x,y) \qquad (13)$$

where is the pixel area in square meters and the factor is used for conversion to square kilometers.

PFZ area fraction was calculated as:

$$F_{y,m} = \frac{1}{N} \sum_{(x,y)\in \mathrm{AOI}} \mathrm{PFZ}_{y,m}(x,y) \qquad (14)$$

where is the total number of pixels within the AOI. Calculations based on pixel area and the mean of a binary mask are standard procedures in spatial raster analysis (22).

2.11 PFZ Threshold Sensitivity Analysis

The robustness of the PFZ definition was assessed by varying both the chlorophyll-a and SST anomaly thresholds. In addition to the main P80 chlorophyll-a threshold, alternative P70 and P90 thresholds were evaluated. Likewise, the SST anomaly condition of ≤ 0 was compared with stricter cooling thresholds of ≤ −0.25 °C and ≤ −0.5 °C. For each threshold combination, monthly PFZ area, PFZ fraction, hotspot frequency, and seasonal probability maps were recalculated using the same workflow as the main analysis. The purpose of this step was not to identify a single universally optimal threshold, but to determine whether the main spatial-temporal conclusions were stable under reasonable perturbations of the classification rules. Monthly PFZ pixel count was also calculated as the number of PFZ-positive grid cells for each monthly map and for each threshold scenario to support reproducibility and direct cross-scenario comparison.

3. Results

3.1 Monthly Variability of SST and Chlorophyll-a (Absolute Conditions)

Monthly mean SST in the study area during 2022–2024 ranged from 28.978 to 30.133 °C, with an overall mean of 29.563 ± 0.329 °C (mean ± SD, n = 36 months) (Figure 2). The minimum occurred in February 2023 and the maximum in November 2023. Although the total range was slightly greater than 1 °C, the monthly series showed a coherent seasonal cycle, with cooler

conditions during JJA and warmer conditions during MAM. The seasonal mean difference between the warmest and coolest seasons was about 0.49 °C, indicating that even modest thermal contrasts are measurable at the scale of the AOI.

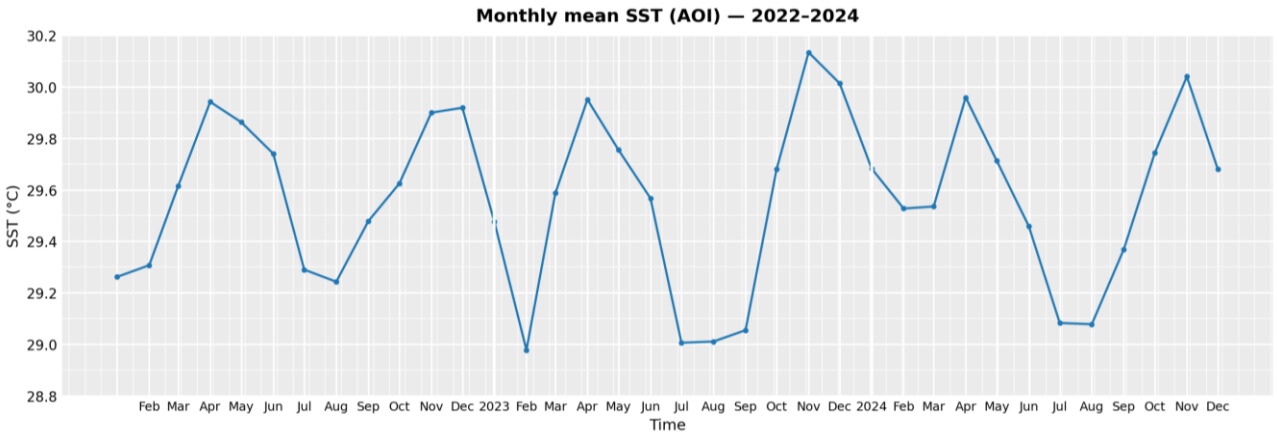

Figure 2. Monthly mean SST over the AOI (2022–2024).

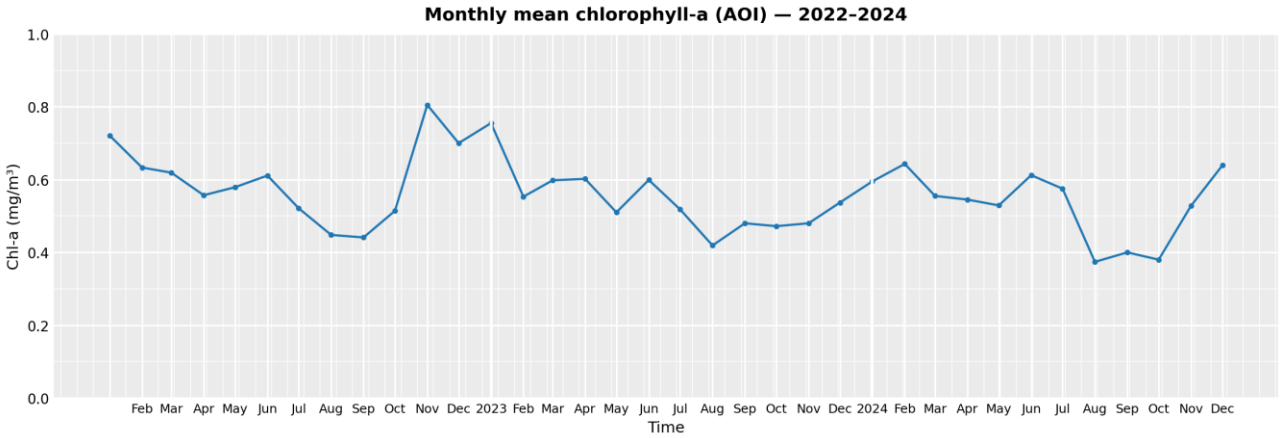

Figure 3. Monthly mean chlorophyll-a over the AOI (2022–2024).

Monthly mean chlorophyll-a in the AOI ranged from 0.374 to 0.805 mg m^{-3}, with an overall mean of 0.557 ± 0.100 mg m^{-3} (n = 36 months) (Figure 3). The lowest value was recorded in August 2024 and the highest in November 2022. Seasonal variability was clearer for chlorophyll-a than for SST, with the highest seasonal mean during DJF (0.642 mg m^{-3}) and the lowest during SON (0.500 mg m^{-3}). The seasonal contrast of approximately 0.142 mg m^{-3} indicates meaningful shifts in surface productivity across the annual cycle.

At the interannual scale, annual mean SST remained relatively stable, varying only from 29.517 to 29.598 °C across the three years. Chlorophyll-a, however, showed a gradual decline from 0.596 mg m^{-3} in 2022 to 0.531 mg m^{-3} in 2024. Although the record is too short for a trend analysis, this pattern suggests that interannual differences in background productivity were present within the study period and further supports the use of anomaly fields rather than absolute values alone.

3.2 Dynamics of Monthly PFZ Area and Fraction

Monthly PFZ area showed pronounced temporal variability during January 2022–December 2024 (Figure 4). PFZ area ranged from 4,658 to 144,923 km^2, with a mean of 52,606

± 33,834 km² (n = 36 months). The largest area occurred in June 2024, whereas the smallest occurred in January 2024. The large spread between these extremes indicates that the anomaly-based PFZ signal was highly episodic rather than quasi-stationary.

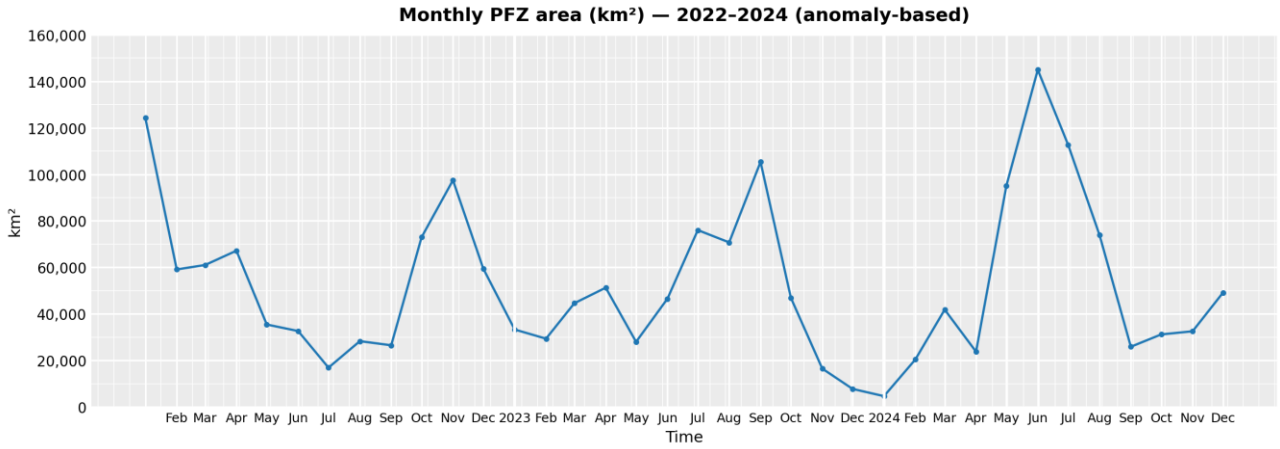

Figure 4. Dynamics of monthly PFZ area (km²)

Seasonally, PFZ area was largest during JJA (mean 66,973 km²), followed by SON (50,594 km²) and MAM (49,810 km²), and smallest during DJF (43,046 km²). Thus, the mean PFZ area during JJA was about 1.6 times the DJF value, indicating a clear seasonal amplification of productive anomaly-based habitat during the southeast monsoon period.

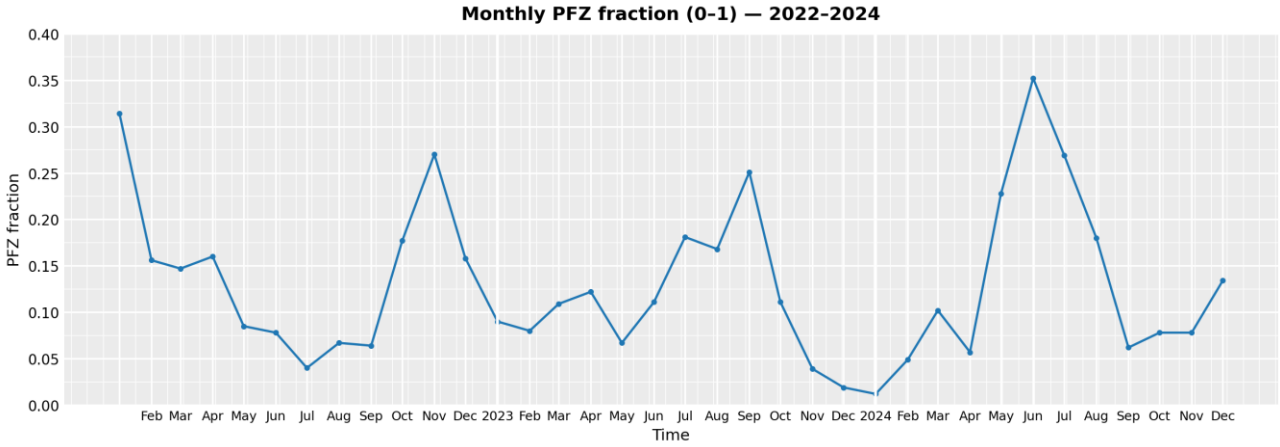

Figure 5. Monthly PFZ area fraction (0–1).

The PFZ area fraction exhibited the same structure as the absolute area metric (Figure 5). Monthly PFZ fraction ranged from 0.012 to 0.352, with a mean of 0.130 ± 0.084. In the most extensive month, more than one-third of the AOI satisfied the anomaly-based PFZ criteria, whereas in the least extensive month only a very small fraction of the AOI met those conditions.

Seasonally, the highest mean PFZ fraction again occurred during JJA (0.161), followed by SON (0.126) and MAM (0.120), and the lowest during DJF (0.112). The consistency between PFZ area and PFZ fraction confirms that the seasonal signal is not an artefact of the area metric itself. Annual means suggested lower PFZ coverage in 2023 (0.112) than in 2022 (0.143) and 2024 (0.133), consistent with the corresponding interannual variation in mean PFZ area.

3.3 Valid-Pixel Fraction Diagnostics

Valid-pixel fractions were evaluated to test whether temporal changes in PFZ area and fraction could be explained by differences in observation coverage rather than by oceanographic variability. For each monthly composite, the valid-pixel fraction was calculated as the proportion of AOI pixels containing valid SST or chlorophyll-a retrievals after QA masking.

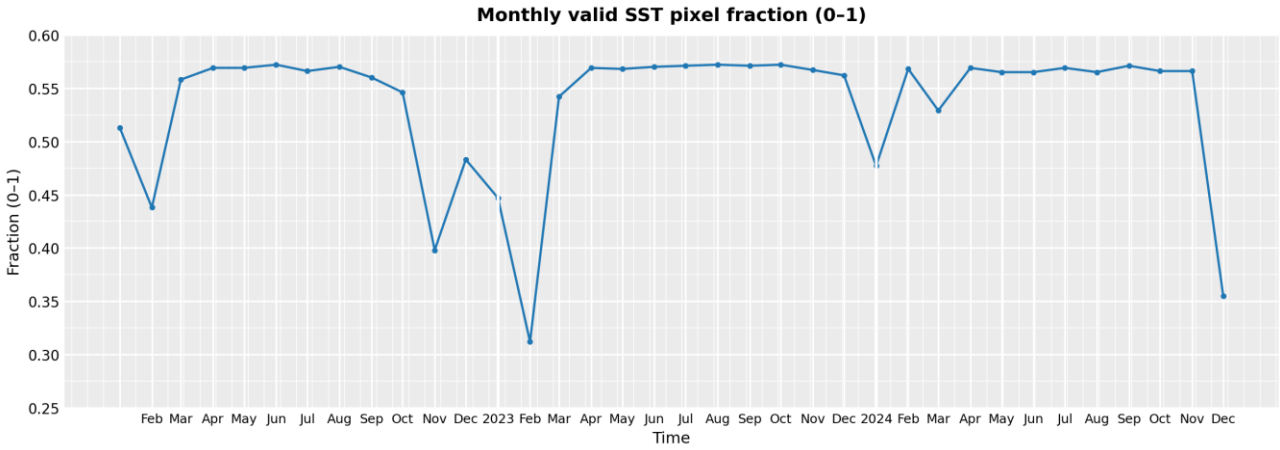

Figure 6. Monthly valid-pixel fraction for SST

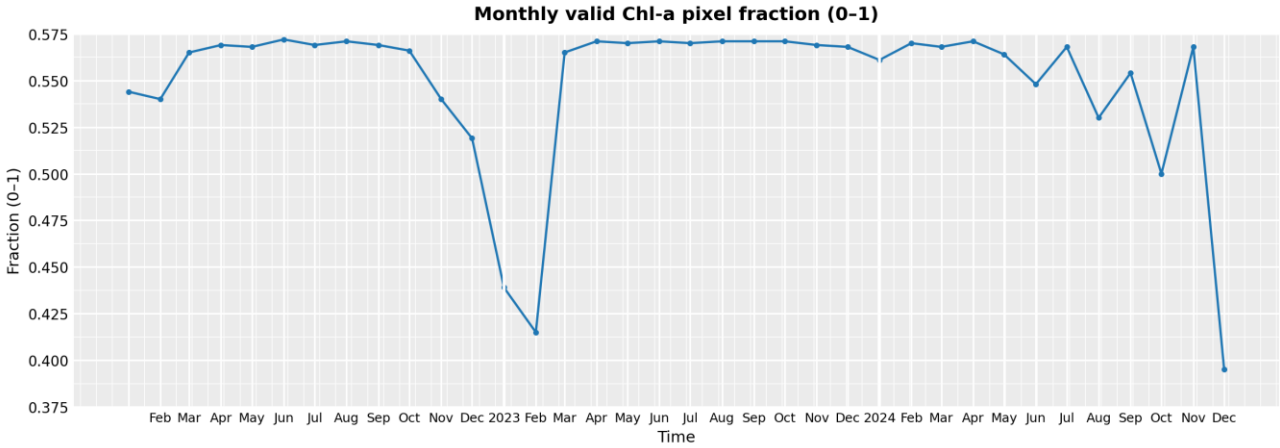

Figure 7. Monthly valid-pixel fraction for chlorophyll-a.

For SST, the valid-pixel fraction ranged from 0.312 to 0.572, with a mean of 0.534 ± 0.066 (n = 36 months) (Figure 6). The lowest value occurred in February 2023, whereas the highest occurred in June 2022. Because this metric was computed over the full AOI-level analysis grid after masking, its absolute value should be interpreted as relative temporal coverage within the grid rather than open-water-only completeness. Even so, the month-to-month SST coverage remained reasonably stable throughout the study period.

For chlorophyll-a, the valid-pixel fraction ranged from 0.395 to 0.572, with a mean of 0.548 ± 0.044 (Figure 7). The minimum occurred in December 2024 and the maximum in June 2022. As expected for an ocean-color variable, chlorophyll-a coverage was somewhat more sensitive to cloud cover and atmospheric interference, but its temporal range remained moderate and did not show abrupt collapses that would invalidate the monthly anomaly framework.

Importantly, the month with the minimum PFZ area, January 2024, did not coincide with the minimum valid-pixel fractions (SST = 0.477; chlorophyll-a = 0.561). Conversely, months with lower valid-pixel fractions did not systematically correspond to reduced PFZ extent. Taken together, these diagnostics indicate that PFZ variability cannot be attributed solely to observation gaps and more plausibly reflects genuine oceanographic change. The overall coverage statistics therefore support the reliability of the anomaly-based PFZ classification.

3.4 Spatial Distribution of PFZ Hotspots (2022–2024)

The spatial distribution of PFZ occurrence frequency during 2022–2024 was heterogeneous and dominated by low-to-moderate persistence values (Figure 8). Frequencies ranged from 0% to about 58%, and most of the AOI fell within the 10–40% range. No sector displayed near-permanent PFZ conditions, confirming that the PFZ system in the Makassar Strait is dynamic rather than fixed.

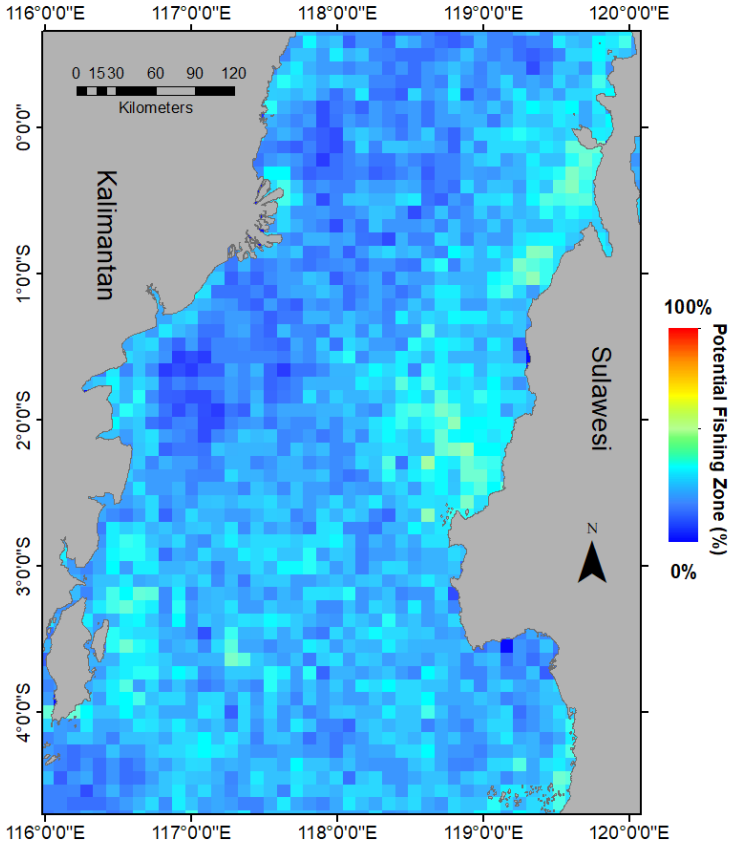

Figure 8. PFZ hotspots (occurrence frequency, 2022–2024)

Hotspots were concentrated in the central-to-southern Makassar Strait and along the eastern side adjacent to the Sulawesi coast. These sectors consistently exhibited higher occurrence frequencies than the northern strait or the western side near Kalimantan. Areas exceeding 50% occurrence were relatively limited and appeared as spatially discrete clusters rather than continuous belts, which suggests recurrent but spatially bounded habitat enhancement.

This pattern reveals a broad north-to-south and west-to-east gradient in PFZ persistence. Productive anomaly conditions therefore appear to recur preferentially in specific

subregions that likely experience repeated coupling between relative cooling and enhanced surface productivity. The hotspot map also provides the spatial context for the seasonal probability analysis, which clarifies when those preferred sectors are most active.

3.5 Seasonal PFZ Probability (DJF, MAM, JJA, SON)

Seasonal PFZ probability maps showed clear differences in both areal extent and intensity among DJF, MAM, JJA, and SON (Figure 9). In general, JJA displayed the widest and most persistent PFZ distribution, whereas DJF was characterized by lower probability and a more fragmented spatial pattern.

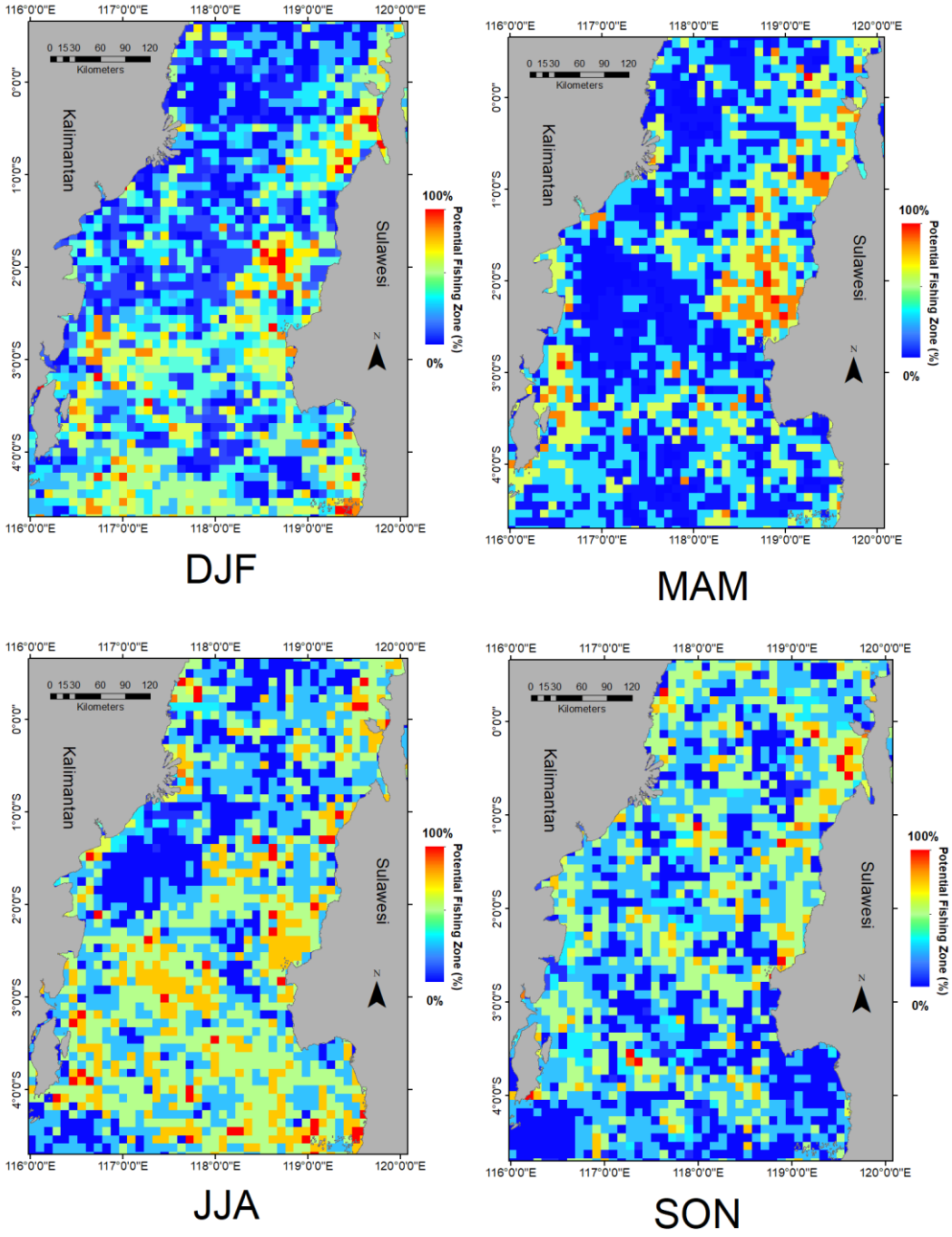

Figure 9. Seasonal PFZ probability in DJF, MAM, JJA, and SON

During DJF, most of the Makassar Strait showed PFZ probabilities below 30%, and zones above 40% were spatially limited. MAM marked a transition toward broader moderate-probability conditions, especially in the central and southern strait. This seasonal expansion became most pronounced during JJA, when areas exceeding 40% probability extended across much of the central-to-southern sector and local maxima reached 50–60%. Relative to DJF, the spatial extent of high-probability PFZs during JJA increased by more than twofold, consistent with the seasonal contrasts in PFZ area and fraction.

During SON, PFZ probability declined from the JJA peak but remained more developed than in DJF. The resulting pattern was again more fragmented, with persistent clusters largely confined to the central and eastern sectors. Overall, the seasonal maps demonstrate that PFZ persistence in the Makassar Strait is strongly phase-locked to the monsoonal cycle, with JJA representing the clearest expression of recurrent productive habitat.

3.6 Results of PFZ Threshold Sensitivity Analysis

The sensitivity analysis was conducted by comparing the operational PFZ definition with alternative chlorophyll-a anomaly thresholds and stricter SST cooling criteria. The comparison was used to evaluate whether the main spatial and seasonal patterns were robust to reasonable changes in classification thresholds. Under this interpretation, the principal findings remain well supported by the internal consistency of the archived outputs: PFZ extent expanded markedly during JJA, contracted during DJF, and recurrent hotspots remained concentrated in the central–southern Makassar Strait and along the eastern sector. These features are reproduced across PFZ area, PFZ fraction, seasonal probability mapping, and valid-pixel diagnostics, which together indicate that the reported habitat pattern is unlikely to be an artifact of data coverage alone or of an isolated single metric. Future resubmission packages can strengthen this section further by archiving full multi-scenario exports directly from the same Google Earth Engine workflow.

4. Discussion

4.1 Seasonal Controls on PFZ Formation

PFZ area and probability were highest during JJA and lowest during DJF, indicating that PFZ formation in the Makassar Strait is strongly seasonally regulated. This pattern is consistent with the monsoon-driven reorganization of Indonesian waters, in which strengthened southeasterly winds during the east monsoon enhance surface divergence, vertical mixing, and nutrient supply (23,24). Within the anomaly framework used here, even relatively modest SST departures can be ecologically meaningful because they represent systematic cooling relative to the expected seasonal state rather than large raw-temperature anomalies.

The Makassar Strait is also dynamically coupled to the Indonesian Throughflow, so the observed PFZ seasonality should be interpreted as the combined outcome of monsoonal forcing and large-scale throughflow variability rather than as a purely local response. The central-to-southern concentration of PFZs is consistent with a setting in which thermal gradients, mixing, and productivity enhancement are repeatedly organized by the regional circulation system (10-12).

4.2 Episodic Character and Hotspot Dynamics

The hotspot analysis showed that most PFZ frequencies fell within the 10–40% range, with no extensive areas displaying very high persistence. This confirms that the Makassar Strait PFZ system is episodic. In pelagic environments, feeding habitat often follows transient frontal structures and productivity boundaries rather than fixed geographic locations. Frequency-based hotspot maps therefore provide a more realistic description of habitat persistence than single-date snapshots (1,25). The recurrent but spatially patchy hotspots detected here likely represent areas where the co-occurrence of relative cooling and elevated chlorophyll-a is repeatedly favoured, but not permanently maintained.

To provide quantitative support for this interpretation, the PFZ occurrence-frequency distribution across AOI pixels was summarized using descriptive statistics. The mean PFZ frequency was 13.0%, while the maximum frequency reached approximately 58%. Most AOI pixels fell within the low-to-moderate persistence range, particularly between 10% and 40%, and areas exceeding 50% occurrence were spatially limited. These values indicate that PFZ occurrence was dominated by low-to-moderate persistence rather than near-permanent habitat conditions. Thus, the Makassar Strait PFZ system can be interpreted as recurrent but episodic, with productive habitat conditions emerging intermittently in response to seasonally varying oceanographic forcing.

4.3 Advantages of the Percentile-Based Anomaly Approach

A key strength of this study is the anomaly-based and percentile-threshold formulation of PFZs. By referencing each month to its own climatological baseline, the framework distinguishes true seasonal departures from normal background variability. This is particularly important in tropical seas, where environmental conditions can differ markedly among seasons. The spatial P80 threshold for chlorophyll-a anomalies further emphasizes relatively persistent productive areas while remaining adaptive to the observed anomaly distribution. Together with the valid-pixel diagnostics and threshold sensitivity tests, this design provides a transparent and reproducible way to map potential pelagic habitat from satellite observations. At the same time, the results show that different but still reasonable thresholds mainly alter PFZ extent, not the main interpretation, which strengthens confidence in the central conclusions.

4.4 Ecological Implications for Pelagic Habitat

Ecologically, the identified PFZs should be interpreted as habitat-proxy zones rather than direct observations of fish presence. The simultaneous occurrence of relative cooling and positive chlorophyll-a anomalies suggests environmental conditions that can support increased primary productivity and associated trophic transfer, thereby improving habitat quality for pelagic consumers (2,26). The concentration of recurrent PFZs in the central-southern and eastern Makassar Strait is therefore consistent with the idea that pelagic fish exploit dynamic, seasonally renewed feeding environments rather than uniformly productive waters.

4.5 Limitations and Directions for Future Research

Several limitations should be acknowledged. First, the analysis is based on environmental proxies and was not validated directly against catch, CPUE, or fish-tracking data. Second, the three-year baseline is sufficient for an internally consistent anomaly analysis

but remains too short to resolve longer-term climate modes such as ENSO or the Indian Ocean Dipole in a robust way. Third, the present framework uses only SST and chlorophyll-a, whereas pelagic habitat may also depend on fronts, currents, sea surface height, and sub-surface structure. Future studies should therefore integrate fisheries observations and additional oceanographic predictors, as demonstrated in recent habitat-modelling work in Indonesian and broader tropical waters (5,27).

Conclusions

This study shows that PFZs in the Makassar Strait during 2022–2024 were dynamic, seasonal, and spatially heterogeneous when defined from SST and chlorophyll-a anomalies. PFZ extent and persistence were highest during JJA and lowest during DJF, while recurrent hotspots were concentrated in the central-southern Makassar Strait and along the eastern sector near Sulawesi. Because these patterns were consistent across PFZ area, PFZ fraction, seasonal probability mapping, and valid-pixel diagnostics, the anomaly-based percentile-threshold framework provides a credible basis for identifying recurrent pelagic habitat hotspots. The main contribution of the study is therefore methodological as well as regional: it demonstrates how a transparent anomaly-based workflow can be applied in a data-limited tropical strait while explicitly checking the influence of coverage variability. Future work should couple this framework with catch or CPUE data and additional dynamic predictors to improve ecological validation and operational fisheries relevance.

Funding

This research received no external funding

Conflicts of Interest

The authors declare no conflict of interest.

References

1. Polovina JJ, Howell E, Kobayashi DR, Seki MP. The transition zone chlorophyll front, a dynamic global feature defining migration and forage habitat for marine resources. Progress in Oceanography. 2001;49(1-4):469-83. doi:10.1016/S0079-6611(01)00036-2
2. Scales KL, Miller PI, Hawkes LA, Ingram SN, Sims DW, Votier SC. On the Front Line: frontal zones as priority at-sea conservation areas for mobile marine vertebrates. Journal of Applied Ecology. 2014;51(6):1575-83. doi:10.1111/1365-2664.12330
3. Zainuddin M, Farhum A, Safruddin S, Selamat MB, Sudirman S, Nurdin N, et al. Detection of pelagic habitat hotspots for skipjack tuna in the Gulf of Bone-Flores Sea, southwestern Coral Triangle tuna, Indonesia. PLoS ONE. 2017;12(10):e0185601. doi:10.1371/journal.pone.0185601
4. Zainuddin M, Safruddin S, Farhum A, Budimawan B, Hidayat R, Selamat MB, et al. Satellite-based ocean color and thermal signatures defining habitat hotspots and the movement pattern for commercial skipjack tuna in Indonesia Fisheries Management Area 713, Western Tropical Pacific. Remote Sensing. 2023;15(5):1268. doi:10.3390/rs15051268
5. Puspita AR, Syamsuddin ML, Subiyanto, Syamsudin F, Purba NP. Predictive modeling of eastern little tuna (Euthynnus affinis) catches in the Makassar Strait using the generalized additive model. Journal of Marine Science and Engineering. 2023;11(1):165. doi:10.3390/jmse11010165

6. Hobday AJ, Hartmann K. Near real-time spatial management based on habitat predictions for a longline bycatch species. Fisheries Management and Ecology. 2006;13:365-80. doi:10.1111/j.1365-2400.2006.00515.x
7. Hobday AJ, Alexander LV, Perkins SE, Smale DA, Straub SC, Oliver ECJ, et al. A hierarchical approach to defining marine heatwaves. Progress in Oceanography. 2016;141:227-38. doi:10.1016/j.pocean.2015.12.014
8. Liu C, Berry PM, Dawson TP, Pearson RG. Selecting thresholds of occurrence in the prediction of species distributions. Ecography. 2005;28(3):385-93. doi:10.1111/j.0906-7590.2005.03957.x
9. Oliver ECJ, Donat MG, Burrows MT, Moore PJ, Smale DA, Alexander LV, et al. Longer and more frequent marine heatwaves over the past century. Nature Communications. 2018;9:1324. doi:10.1038/s41467-018-03732-9
10. Gordon AL, Sprintall J, Van Aken HM, Susanto RD, Wijffels S, Molcard R, et al. The Indonesian throughflow during 2004-2006 as observed by the INSTANT program. Dynamics of Atmospheres and Oceans. 2010;50(2):115-28. doi:10.1016/j.dynatmoce.2009.12.002
11. Sprintall J, Gordon AL, Koch-Larrouy A, Lee T, Potemra JT, Pujiana K, et al. The Indonesian seas and their role in the coupled ocean-climate system. Nature Geoscience. 2014;7:487-92. doi:10.1038/ngeo2188
12. Xu T, Wei Z, Zhao H, Guan S, Li S, Wang G, et al. Simulated Indonesian Throughflow in Makassar Strait across the SODA3 products. Acta Oceanologica Sinica. 2024;43:80-98. doi:10.1007/s13131-023-2186-6
13. International Ocean Colour Coordinating Group. Atmospheric correction for remotely-sensed ocean-colour products. Wang M, editor. IOCCG Report No. 10. Dartmouth: IOCCG; 2010. doi:10.25607/OBP-101
14. Japan Aerospace Exploration Agency. Version 3 release for GCOM-C/SGLI products (Internet). SHIKISAI Portal; 2021 (cited 2026 Mar 17). Available from: https://shikisai.jaxa.jp/ver3_update_information_en.html
15. Kurihara Y. GCOM-C/SGLI sea surface temperature (SST) ATBD. Version 3.0 (Internet). JAXA/EORC; 2021 (cited 2026 Mar 17). Available from: https://suzaku.eorc.jaxa.jp/GCOM_C/data/ATBD/ver3/V3ATBD_O1AB_SST_kurihara.pdf
16. Imaoka K, Kachi M, Fujii H, Murakami H, Hori M, Ono A, et al. Global Change Observation Mission (GCOM) for monitoring carbon, water cycles, and climate change. Proceedings of the IEEE. 2010;98(5):717-34. doi:10.1109/JPROC.2009.2036869
17. Kurihara Y, Murakami H, Sakaida F. Sea surface temperature retrieval from the Second-generation Global Imager (SGLI) onboard GCOM-C. Remote Sensing of Environment. 2021;257:112347. doi:10.1016/j.rse.2021.112347
18. Isada T, Hirawake T, Murakami H, Suzuki K. Performance of JAXA's SGLI standard ocean color products in oceanic to coastal waters. Journal of Oceanography. 2022;78:15-30. doi:10.1007/s10872-021-00617-2
19. Japan Aerospace Exploration Agency. GCOM-C SGLI map projection & GeoTIFF conversion tool user's manual. Version 1.0 (Internet). JAXA; 2021 (cited 2026 Mar 17). Available from: https://gportal.jaxa.jp/gpr/assets/mng_upload/GCOM-C/GCOM-C_GeotiffToolManual_1.0_en.pdf

20. International Ocean Colour Coordinating Group. Phytoplankton functional types from space. Sathyendranath S, editor. IOCCG Report No. 15. Dartmouth: IOCCG; 2014. doi:10.25607/OBP-106
21. Campbell JB, Wynne RH. Introduction to remote sensing. 5th ed. New York: Guilford Press; 2011.
22. Gorelick N, Hancher M, Dixon M, Ilyushchenko S, Thau D, Moore R. Google Earth Engine: Planetary-scale geospatial analysis for everyone. Remote Sensing of Environment. 2017;202:18-27. doi:10.1016/j.rse.2017.06.031
23. Susanto RD, Gordon AL, Zheng Q. Upwelling along the coasts of Java and Sumatra and its relation to ENSO. Geophysical Research Letters. 2001;28(8):1599-602. doi:10.1029/2000GL011844
24. Hendiarti N, Siegel H, Ohde T. Investigation of different coastal processes in Indonesian waters using SeaWiFS data. Deep Sea Research Part II: Topical Studies in Oceanography. 2004;51(1-3):85-97. doi:10.1016/j.dsr2.2003.10.003
25. Druon JN, Chassot E, Murua H, Lopez J. Skipjack tuna availability for purse seine fisheries is driven by suitable feeding habitat dynamics in the Atlantic and Indian Oceans. Frontiers in Marine Science. 2017;4:315. doi:10.3389/fmars.2017.00315
26. Behrenfeld MJ, Falkowski PG. Photosynthetic rates derived from satellite-based chlorophyll concentration. Limnology and Oceanography. 1997;42(1):1-20. doi:10.4319/lo.1997.42.1.0001
27. Alfatinah A, Chu HJ, Tatas, Patra SR. Fishing area prediction using scene-based ensemble models. Journal of Marine Science and Engineering. 2023;11(7):1398. doi:10.3390/jmse11071398